Available online at www.sciencedirect.com
SCIENCE DIRECT®
International Journal of Mass Spectrometry 244 (2005) 29–40
International Journal of Mass Spectrometry
www.elsevier.com/locate/ijms

Fragmentations and reactions of some isotopically labelled dimethyl methyl phosphono and trimethyl phosphoro thiolates and thionates studied by electrospray ionisation ion trap mass spectrometry

J.D. Barr [a,b], A.J. Bell [c], F. Ferrante [d], G. La Manna [d], J.L. Mundy [c], C.M. Timperley [c], M.J. Waters [c], P. Watts [c,*]

[a] *Department of Chemistry, Southampton University, Southampton SO7 1BJ, UK*
[b] *Institut Català d'Investigació Química (ICIQ), Av. Paisos, Catalans, s/n, 43007 Tarragona, Spain*
[c] *Dstl Porton Down, Salisbury, Wilts SP4 0JQ, UK*
[d] *Dipartimento di Chimica Fisica "F. Accascina", Università, degli Studi di Palermo, 90128 Palermo, Italy*

Received 23 February 2005; accepted 12 April 2005
Available online 13 May 2005

Abstract

In this paper, studies on electrospray ionisation ion trap mass spectrometry of organophosphates are extended to a series of dimethyl methylphosphono and trimethyl phosphoro thionates and thiolates and some deuterated isotopomers. Of particular, interest is the comparison of the collision-induced fragmentation of ions from these compounds with those of the non-sulphur containing analogues reported previously. The thiono and thiolo isomeric structures of the sulphur containing ions analogous to **I** and **II** (see below) have very similar energies and undergo a ready interconversion. In the case of the phosphono compounds, the electronic structure calculations show that the methyl migration implicit in thiono–thiolo interconversion occurs directly and although methyl migration from P to the phosphonyl O or phosphonothionyl S can occur, the transition state (TS) energies are somewhat higher and, in the case of the migration to O, too high to take part in any of the subsequent collision induced fragmentations. With one exception, the mechanisms proposed for some of these fragmentations are supported by electronic structure calculations at the DFT-B3LYP level.

Keywords: Mass spectrometry; Electrospray; Ion trap; Organophosphates; Thiono–thiolo rearrangement

1. Introduction

A previous study [1] demonstrated that formaldehyde was eliminated on fragmentation of the ions **I** and **II** in an ion trap mass spectrometer.

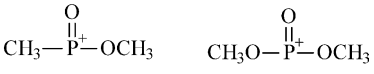

I **II**

These ions were formed by fragmentation of protonated dimethyl methylphosphonate and trimethyl phosphate, respectively. It was also shown that the methyl groups in **I** undergo partial scrambling before the elimination of formaldehyde. As a result of further studies [2] on **I**, it was suggested that 1,4-H migrations to oxygen occurred. Subsequent electronic structure calculations at the B3LYP and MP2 levels showed however that 1,4-H migrations to oxygen were energetically unfavourable and that 1,3-H migrations to phosphorus were preferred [3]. The present paper reports a study of the fragmentation of the corresponding phosphono and phosphoro thiolates and thionates (structures **III**–**IX**).

* Corresponding author. Tel.: +44 1980 862161; fax: +44 1980 863904.
E-mail address: pwatts.rsg@ukgateway.net (P. Watts).

1387-3806/$ – see front matter © 2005 Elsevier B.V. All rights reserved.
doi:10.1016/j.ijms.2005.04.004

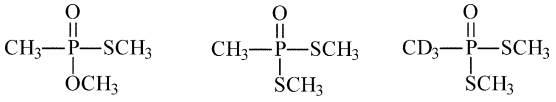

III **IV** **V**

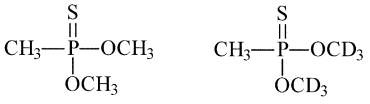

VI **VII**

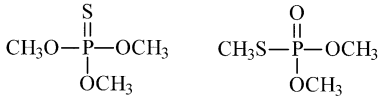

VIII **IX**

This work (which is part of a larger study) also underpins our investigations of more complex organophosphates [4,5] and is of potential relevance to an understanding of thiono–thiolo rearrangments of phosphorus esters.

Thiono–thiolo rearrangement, where the S=P–OR group rearranges to the O=P–SR group, can be effected by alkylating agents or by acids, by heating or by electron ionisation. When R is a proton, the position of equilibrium depends on the alkylating agent and the solvent. Methylation of diethyl phosphorothioate with diazomethane in ether gave a 1:4 mixture of $(EtO)_2P(S)OMe$ and $(EtO)_2P(O)SMe$ [6]. This reflects the higher affinity of the sulphur atom, a soft base [7], for the carbon atom of diazomethane, a soft acid. Such reactivity preferences control the outcome of all thiono–thiolo rearrangements. When R is an alkyl group, rearrangement can occur when the thiono compounds are heated with alkyl halides, a process known as the Pishchimuka reaction [8,9]. The mechanism involves attack of the sulphur atom on the carbon atom of the alkyl halide to give a phosphonium salt, then dealkylation of one of the ester groups by the halide ion.

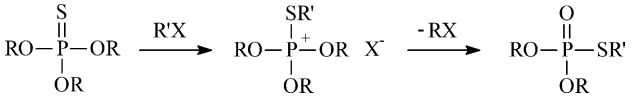

Factors that moderate the rearrangement are the substituents in the thionate and the leaving group of the alkyl halide. The more electron-donating the substituents in the thionate, the greater the nucleophilicity of the thiophosphoryl group. The better the leaving group in the alkyl halide, the faster the reaction; the rate decreases in the order RI > RBr > RCl > RF. A good example of the Pishchimuka reaction is conversion of $(MeO)_2P(S)NH_2$ by methyl iodide to the pesticide Tameron $MeO(MeS)P(O)NH_2$ [8]. The electron-donating amino group in the starting material enhances the nucleophilicity of the sulphur atom and facilitates isomerisation.

Rearrangement can also be catalysed by acids. The same rules of reactivity apply for the phosphorus reagent, but the rate depends on the strength of the acid. Half-lives for rearrangement of $(MeO)_3P=S$, $(MeO)_2P(S)Ph$ and $Ph_2P(S)OMe$ in dilute trifluoroacetic acid were 0.5, 1 and 4 h, respectively, and rearrangement of $(MeO)_3P=S$ was 14 times quicker in trifluoroacetic acid than in trichloroacetic acid [10]. Mixtures of thionates were reported as giving mixed thiolates indicating an intermolecular mechanism. In acid-catalysed rearrangements, protonation of the thiophosphoryl sulphur atom must occur in the first step [10], the mechanism thereafter paralleling that of the Pishchimuka reaction.

Instances of thermal rearrangement probably reflect an acceleration of an isomerism that occurs very slowly at room temperature and which is possibly catalysed by trace amounts of acid arising from the invariable presence of trace amounts of pyrophosphates [11]. Intramolecular rearrangements have been used to make the pesticides Amiton [12] and Systox [13]. The driving force in these reactions is the ease of ionisation of the thiono precursors, which is a result of the stability of the intermediate ethyleniminium or sulfonium ions.

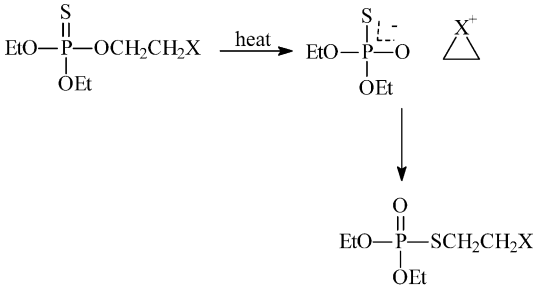

X=NEt_2 Amiton
X=SEt Systox

Rearrangements of simple phosphorothionates require strong heating and rarely result in complete conversion to the thiolate. Rearrangement of $(CH_3O)_3P=S$ to $(CH_3O)_2P(O)SMe$ was only half complete after heating in a sealed tube at 100 °C for several hours [14]. Attack of the thiophosphoryl group takes place on one of the ester groups. The more electrophilic the ester carbon atom, the easier the reaction: $(CH_3O)_3P=S$ rearranges on heating much faster than $(EtO)_3P=S$ [8]. Thermal rearrangements can be regarded as special cases of the Pishchimuka reaction. A detailed study of the thermal/microwave thiono–thiolo system is in progress in our laboratories and preliminary data obtained from a mixture of isotopomers suggests that at least part of the isomerisation goes by an intermolecular mechanism [15].

Thiono–thiolo rearrangements in the gas phase (particularly of even electron ions) have not been studied to any extent, but have been suggested to occur under electron ionisation [16,17] and by isobutene chemical ionisation [18]. This study extends knowledge of the behaviour of small phosphorus–sulphur species in the gas phase, with a view to

establishing rules to predict the fragmentation and rearrangement of more complex analogues. This approach is necessary before the ion trap mass spectra of phosphorus–sulphur pesticides, such as Diazinon in which a thiono–thiolo rearrangement has been found [5], can be properly interpreted, and underpins our previous investigation of the behaviour of the nerve agent VX in the ion trap mass spectrometer [4].

2. Experimental

The mass spectrometric technique has been described in detail elsewhere [2]. In this work only the Esquire∼LC, Bruker Daltonics, GmbH ion trap mass spectrometer was used. The organophosphates were introduced into the ion trap using 1:1 (MeOH:H_2O) + 0.1% formic acid at a concentration of 400 μg ml^{-1}. The sample was introduced into the elctrospray system by direct infusion (using a syringe drive) at 3 μl min^{-1}. The capillary voltage was −4 kV with an endplate offset voltage of −500 V. The drying gas flow rate was 7l min^{-1} at a temperature of 300 °C. All other lenses were optimised for maximum transfer into the trap. The q_z was 0.4, the excitation voltage adjusted to give the required degree of fragmentation using a 30 ms fragmentation time. It should be noted that with the exception of the ions given in brace brackets, {}, all ions were isolated before fragmentation which removed ambiguity in the precursor–fragment ion relationships. Syntheses of the compounds will be described elsewhere [19]. The compounds were greater than 99% pure by analysis by multinuclear NMR spectroscopy (^1H, ^{13}C and ^{31}P).

All electronic structure calculations were performed using the Gaussian 98 programme [20]. DFT-B3LYP calculations were performed with a 6-311 + G(2df, 2p) basis set for all atoms. Details of the methods used are given elsewhere [3]. These earlier studies on ions obtained from protonated dimethyl methylphosphonate demonstrated that the results at the B3LYP level corresponded very well with those from the more time-consuming MP2 calculations.

3. Results

3.1. Thiolo and thiono phosphonates

3.1.1. Compound *III*

On fragmentation, protonated **III** (i.e., **III**H^+) eliminates primarily methanethiol to produce **I** which has been studied in detail elsewhere [2]. A small amount of methanol is also lost to produce an ion with *m/z* 109 which has identical properties to the ion with *m/z* 109 produced from **IV**H^+ and will be discussed later. The primary site for protonation will be the phosphoryl oxygen (proton affinity 895 kJ mol^{-1}) but for fragmentation to occur the proton has to move to the methylthiolo or methoxy groups.

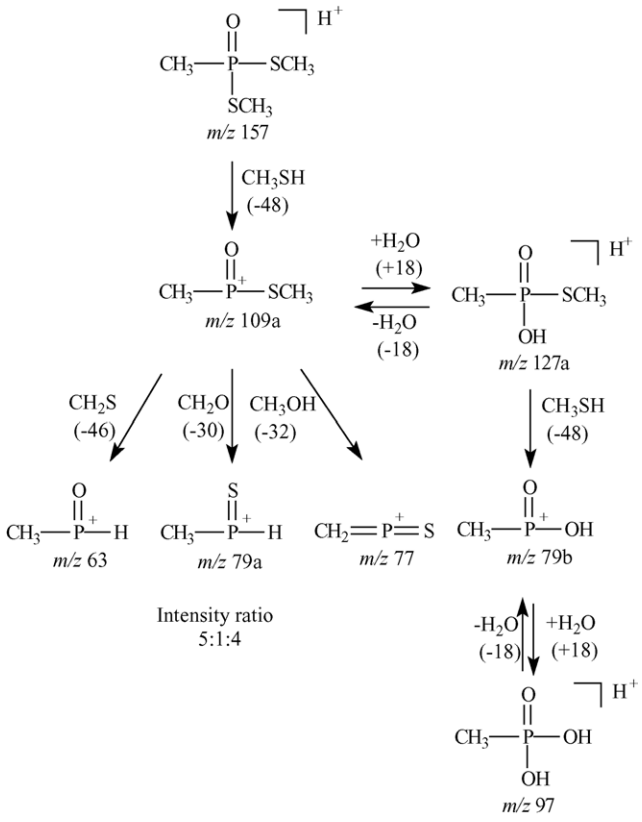

Fig. 1. Fragmentation pathways for protonated **IV**.

3.1.2. Compounds *IV* and *V*

Fragmentation pathways for protonated **IV** and **V** are shown in Figs. 1 and 2, respectively.[1] The fragmentation products of *m/z* 109a produced from **IV**H^+ (Fig. 1) were unexpected, particularly as loss of methanol from the corresponding ion in the fragmentation of dimethyl methylphosphonate was not observed [2]. This stimulated the synthesis and investigation of the isotopically labelled **V**, the fragmentation pathway of which is shown in Fig. 2. This demonstrated the surprising result (in view of the partial scrambling of the methyl groups in **I**, $CH_3P(O)OCH_3^+$, that occurred on fragmentation) that on fragmentation of *m/z* 112a only the carbon from the *S*-methyl group was eliminated in the form of the three carbon containing neutrals. In the fragmentation of *m/z* 112a, no ions resulting from loss of CH_3SD or CD_3SH were observed. The structures assigned to the ions *m/z* 63 and 79a in Fig. 1 (and their deuterated isotopomers in Fig. 2) reflect the probability that they result from a 1,3-

[1] The empirical formulae of the ions given in the fragmentation pathways are, in the main, unambiguous. The associated structures of the ions and neutrals are suggested as being the most reasonable on chemical grounds with particular note being taken of their subsequent fragmentation products; exceptions to this are the positions of the hydrogens and bonding in some of the smaller fragment ions. An ion placed inside brace brackets, {}, has not been detected and its occurrence is assumed on mechanistic grounds.

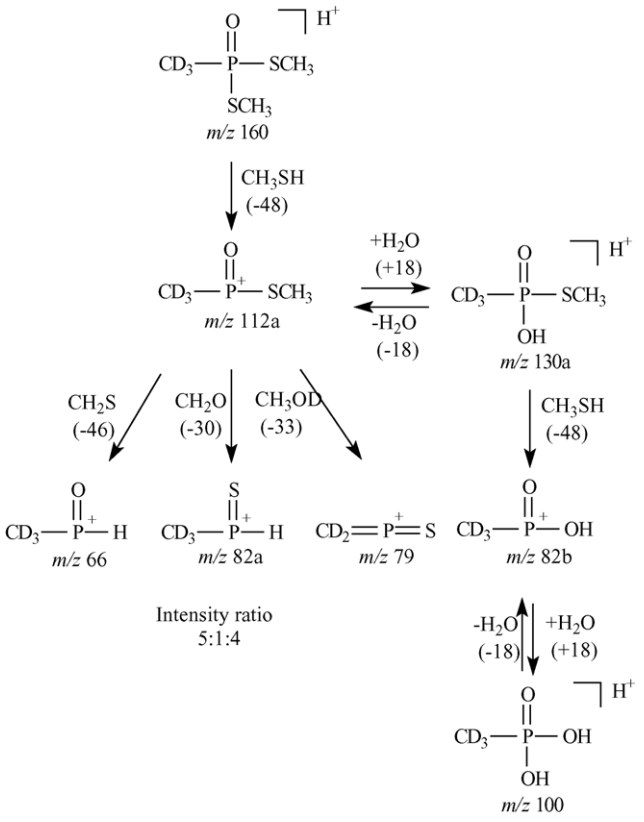

Fig. 2. Fragmentation pathways for protonated **V**.

H shift to phosphorus as in the fragmentation of **I** [3]. The fragmentation of *m/z* 109a (Fig. 1) and *m/z* 109b (Fig. 3) (and their deuterated isotopomers) will be discussed later in conjunction with the results from the electronic structure calculations.

The different structures assigned to *m/z* 79a and b (Fig. 1) and *m/z* 82a and b (Fig. 2) are supported by their different behaviour. On isolation, *m/z* 79a and 82a generated by collision-induced dissociation of *m/z* 109a and 112a respectively, do not react with water to any appreciable extent. Attempts to fragment these small ions were mainly unsuccessful leading primarily to a loss of ions. The deuterated ion *m/z* 82a fragmented with the loss of 19 Da (presumably CD_3H) to give an ion of *m/z* 63 albeit with very low intensity. On isolation, *m/z* 79b and 82b generated by collision-induced dissociation of *m/z* 127a and 130a, respectively, react readily with water which is invariably present in the bath gas. Attempts to fragment *m/z* 79b gave only the water adduct at *m/z* 97 again at very low intensity. This hydration pattern is general in ions having a P=O bond, which add water more easily than the corresponding ions having a P=S bond. For example, the phosphonyl ion *m/z* 109a (Fig. 1) reacted with water after isolation, much more easily than the thiophosphonyl ion *m/z* 109b (Fig. 3, see later). The structures of the ions resulting from the fragmentation of *m/z* 109a will be discussed later.

Only the *S*-methyl group in ions with *m/z* 109a (Fig. 1) and *m/z* 112a (Fig. 2) migrated to the phosphoryl oxygen before fragmentation in contrast with the phosphono methyl group in **I** produced from dimethyl methylphosphonate.

3.1.3. Compounds *VI* and *VII*

Fragmentation pathways for protonated **VI** and **VII** are shown in Figs. 3 and 4, respectively. These compounds were not examined without difficulty, even when stored in a refrigerator they slowly isomerised to the thiolo isomers (see notes on the thiono–thiolo rearrangement in Section 1). Although the small amounts produced could not be detected by NMR techniques, they could be detected by ESI ITMS, presumably because, contrary to published data (see later), the P=O group has a higher proton affinity than the P=S group. Thus, the initial fragmentation spectrum depended upon the age of the sample, so much so that over the course of a year the initial fragmentation spectrum of a sample of **VI** could change from that appropriate to **VI** to that appropriate to **III** with mixed spectra being obtained at intermediate times. It must be stressed that during this time the purity of the sample of **VI** remained unchanged when examined by multinuclear NMR spectroscopy. These findings are important as the first experiments with **VI** were on an old sample, which gave a mixed spectrum, which was interpreted as being indicative of an intramolecular isomerisation, i.e., a thiono–thiolo rearrangement in the gas phase. It was only later that it became apparent that this was not the case and that the fragmentation products resulting from the thiolo form resulted from the trace amounts produced by intermolecular isomerisation in the liquid sample rather than in the gas phase.

Whilst the ions with *m/z* 109a (Fig. 1) and *m/z* 109b (Fig. 3) fragment to give identical products with similar intensities, they are isomeric as their hydration products, *m/z* 127a and b, fragment differently. Thus, *m/z* 109a and b only isomerise to a common structure on collisional activation immediately prior to fragmentation. This isomerisation will be discussed in more detail later. Structurally (equating for the present hydrogen and deuterium), the fragmentation products and their associated intensities from *m/z* 112a are identical to those from *m/z* 109a, indicating no kinetic isotope effect. A similar observation is not made, however, for the corresponding pair of isotopic ions with *m/z* 112b and 109b; although the fragmentation products are the same (equating for the present hydrogen and deuterium as before), the intensities are remarkably different. The identities of the minor product ions from fragmentation of *m/z* 112b (Fig. 4) are ascribed as follows: *m/z* 80 (8%) requires loss of 32 Da (CD_2O), *m/z* 78 (4%) loss of 34 Da (tentatively attributed to H_2S), *m/z* 66 (4%) loss of 46 Da (CH_2S), *m/z* 64 (10%) loss of 48 Da (CD_2S) and *m/z* 63 (12%) loss of 49 Da (CH_3SD). The low intensity of these ions precludes a more detailed investigation at this time. Interestingly, there was no loss of CD_3SH.

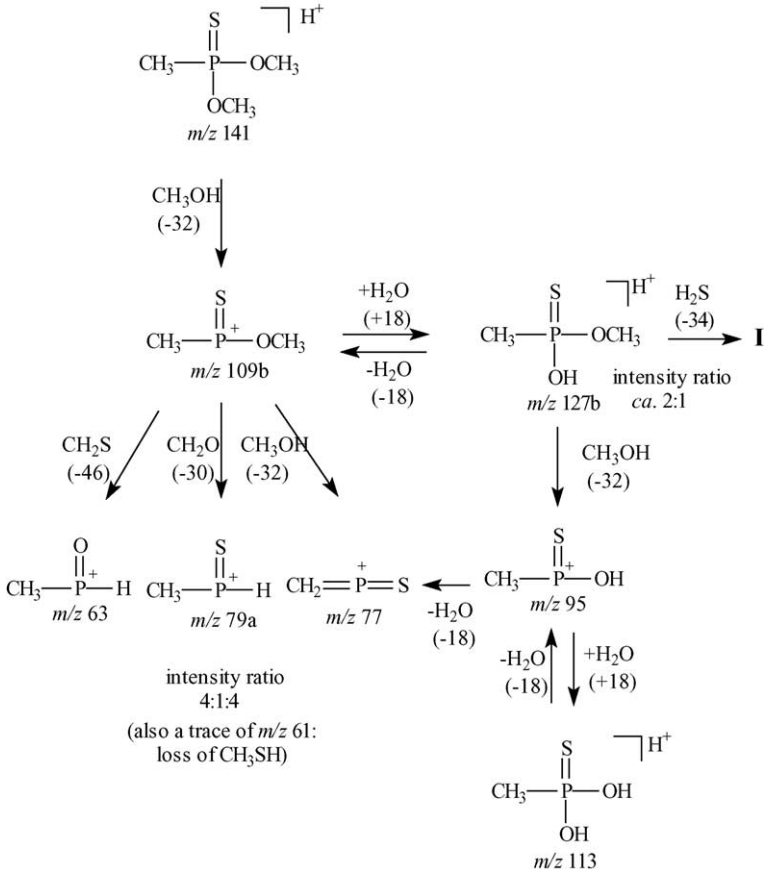

Fig. 3. Fragmentation pathways for protonated **VI**.

3.2. Thiolo and thiono phosphates

3.2.1. Compounds *VIII* and *IX*

As with the phosphonothionate **VI**, problems were encountered with **VIII** due to trace isomerisation to the phosphorothiolate **IX**. This problem was overcome by investigating both **VIII** and **IX** immediately after synthesis (within 24 h). On isolation and fragmentation of MH^+ (*m*/*z* 157) both compounds gave virtually identical mass spectra, not only masses but relative intensities (see Figs. 5 and 6). The initial conclusion was that **VIII**, although freshly prepared, contained traces of the thiolo isomer **IX** and its greater proton affinity compared to **VIII**, enabled it to dominate the ESI process.

This proved not to be the case as isolation and fragmentation of *m*/*z* 143a from **VIII** gave ions with *m*/*z* 111, 113, 125, 127 and 129 (Fig. 7) whereas, *m*/*z* 143b from **IX** only gave ions with *m*/*z* 113, 125 and 129 (Fig. 8).

Additionally, *m*/*z* 125a added water much less readily than did *m*/*z* 125b in accord with the behaviour of the corresponding ions from **IV** to **VI**. Fragmentation pathways for the two compounds are shown in Figs. 9 and 10, respectively. The almost identical mass spectra produced after fragmentation of the protonated starting compounds is fortuitous. Again methyl migration occurs only immediately prior to fragmentation. The structure(s) of *m*/*z* 79 will be discussed later.

3.3. Electronic structure calculations at the DFT-B3LYP level

3.3.1. Thiolo and thiono phosphonates

The proton affinities (PAs) for the basic sites in the thiolate **III** are calculated as 895, 828 and 788 kJ mol^{-1} for the phosphoryl oxygen, the thiol sulphur and the methoxy oxygen, respectively. The PAs for the dithiolate **IV** are calculated as 896 and 823 kJ mol^{-1} for the phosphoryl oxygen and the thiol sulphur, respectively. Similarly, the PAs for the thionate **VI** are calculated as 880 and 789 kJ mol^{-1} for the thiono sulphur and the methoxy oxygens. The thiolate **III** is calculated to be more stable than the isomeric thionate **VI** by 27 kJ mol^{-1} and **III**H^+ to be more stable than **VI**H^+ by 37 kJ mol^{-1} for the lowest energy conformations and the most basic sites.

3.3.2. Thiolo and thiono phosphates

The calculated PAs for the basic sites of the thionate **VIII** are 872 and 779 kJ mol^{-1} for the thiono sulphur and methoxy oxygen, respectively. Those for the thiolate **IX** are 880, 779

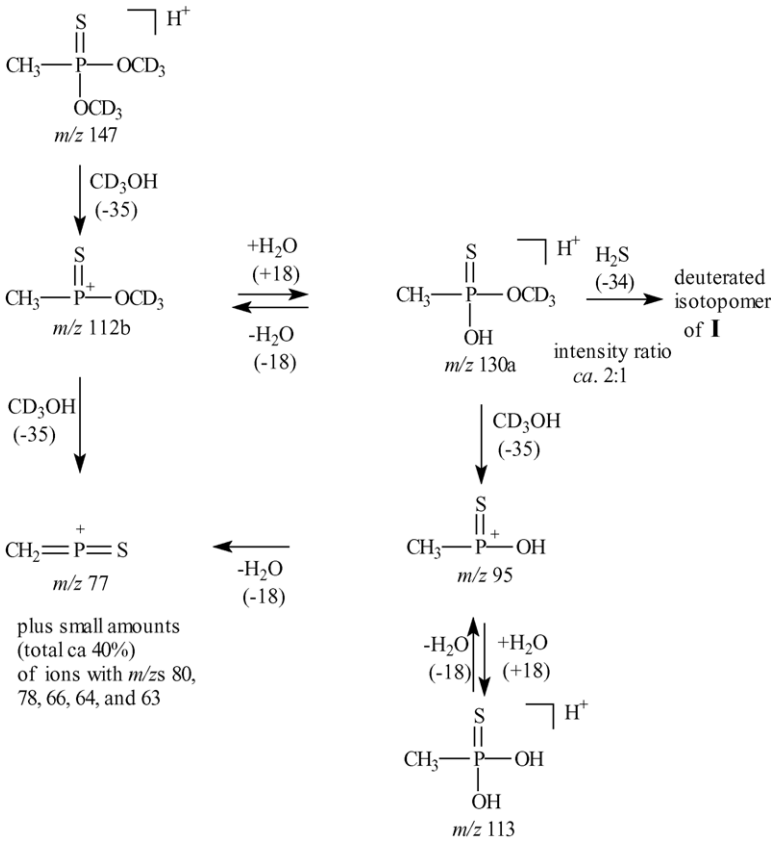

Fig. 4. Fragmentation pathways for protonated **VII**.

and 815 kJ mol^{-1} for the phosphoryl oxygen, the methoxy oxygen and the thiolo sulphur, respectively. For trimethyl phosphate the PAs are 889 and 768 kJ mol^{-1} for the phosphoryl oxygen and the methoxy oxygen, respectively.

The present calculations indicate that the proton affinities of the thiolo isomers (containing the P=O grouping) are greater than those of the thiono isomers (containing the P=S grouping). Although this might be expected on chemical grounds, it is not in accord with values in the NIST data base [21] where similar proton affinities for trimethyl phosphate, $(CH_3O)_3PO$, (891 kJ mol^{-1}) and trimethylphosphorothionate, $(CH_3O)_3PS$ (884 kJ mol^{-1}) are given or with an earlier ICR study by Beauchamp and co-workers [22] where 895 and 905 kJ mol^{-1} were determined for the same compounds. As the present work has shown that, except for very fresh samples of a thiono compound, traces of the thiolo isomer are always present and as Beauchamp and co-workers [22] were using commercial sources, it can be assumed that their

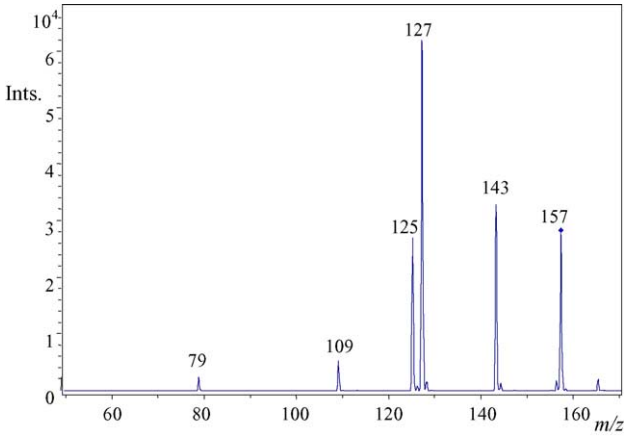

Fig. 5. Fragmentation of MH$^+$ (*m*/*z* 157) from **VIII**.

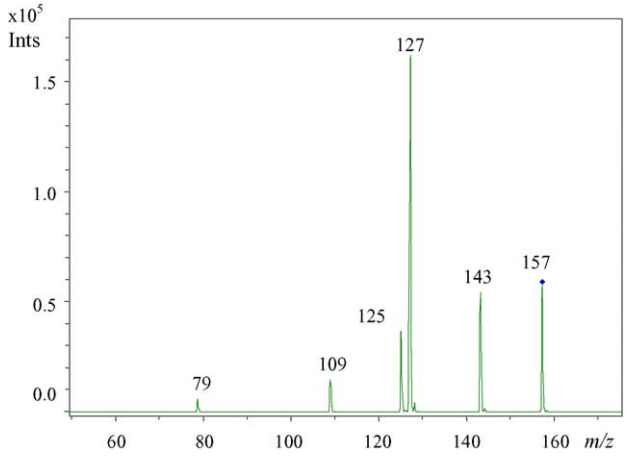

Fig. 6. Fragmentation of MH$^+$ (*m*/*z* 157) from **IX**.

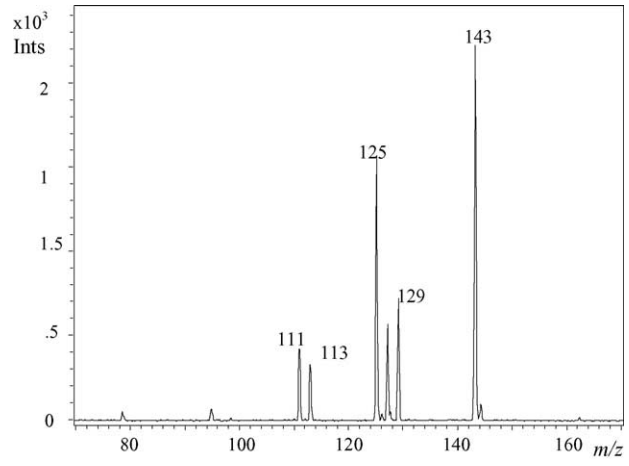

Fig. 7. Fragmentation of *m*/*z* 143a from **VIII**.

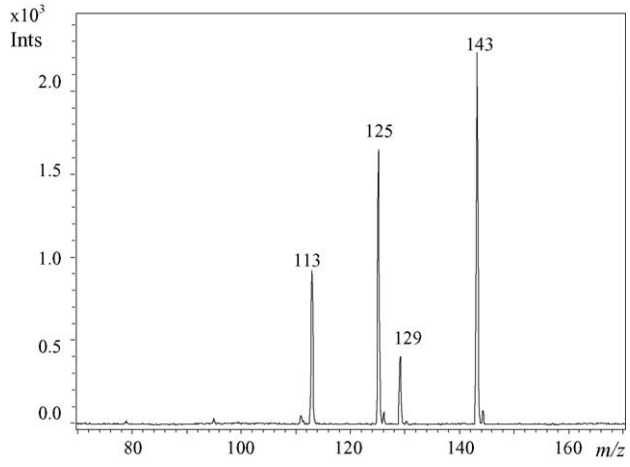

Fig. 8. Fragmentation of *m*/*z* 143b from **IX**.

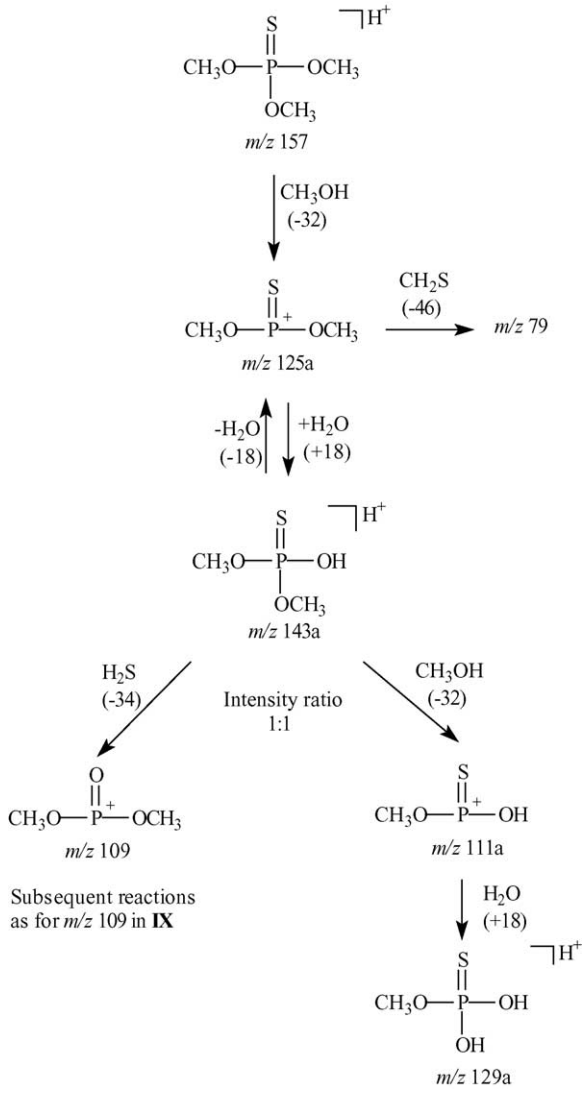

Fig. 9. Fragmentation pathways for protonated **VIII**.

determination pertained not to trimethyl phosphorothionate but to the *O*,*O*,*S*-trimethyl phosphorothiolate that may have been present in their sample.

The relative energies for the various transition states will be given in the discussion of the fragmentations.

4. Discussion

Some preliminary discussion of the fragmentations is valuable when presenting the results. Before a fuller analysis is given, it will be useful to discuss the relationship between fragmentation, isomerisation and energetics in an ion trap although most of this is well known [23]. Until an excitation voltage is applied, all ions in the trap will be at a similar temperature to that of the bath gas (they may be at a slightly elevated temperature due to the influence of the trapping field and there may also be differences between ions with different mass-to-charge ratios, *m*/*z*, due to their different secular frequencies, but these effects are small compared to those of excitation). On excitation, all ions with a particular *m*/*z* will be excited into larger orbits and gain kinetic energy, which will be converted into an increase in internal energy due to collisions with the bath gas. When this gain in internal energy is greater than that of the energy of the transition state (TS) to fragmentation (or the endothermicity of fragmentation if no TS is present) then fragmentation will occur. Consider an ion, A1, excited to an increase in internal energy of 200 kJ mol^{-1}. If the energy of the TS to fragmentation is $\leq$200 kJ mol^{-1} relative to A1, then fragmentation will occur. If it is >200 kJ mol^{-1}, it will not (for simplicity, a Boltzmann distribution of energies is not being taken into account, but this does not affect the argument). Now, consider the case where the A1 does not fragment but can isomerise to an ion, A2 that is 100 kJ mol^{-1} endothermic relative to A1. As before, if the energy of the TS to isomerisation is $\leq$200 kJ mol^{-1}, isomerisation will occur, if greater, it will not. Now, let A2 have a TS energy to fragmentation of 200 kJ mol^{-1} relative to A2 or 300 kJ mol^{-1}

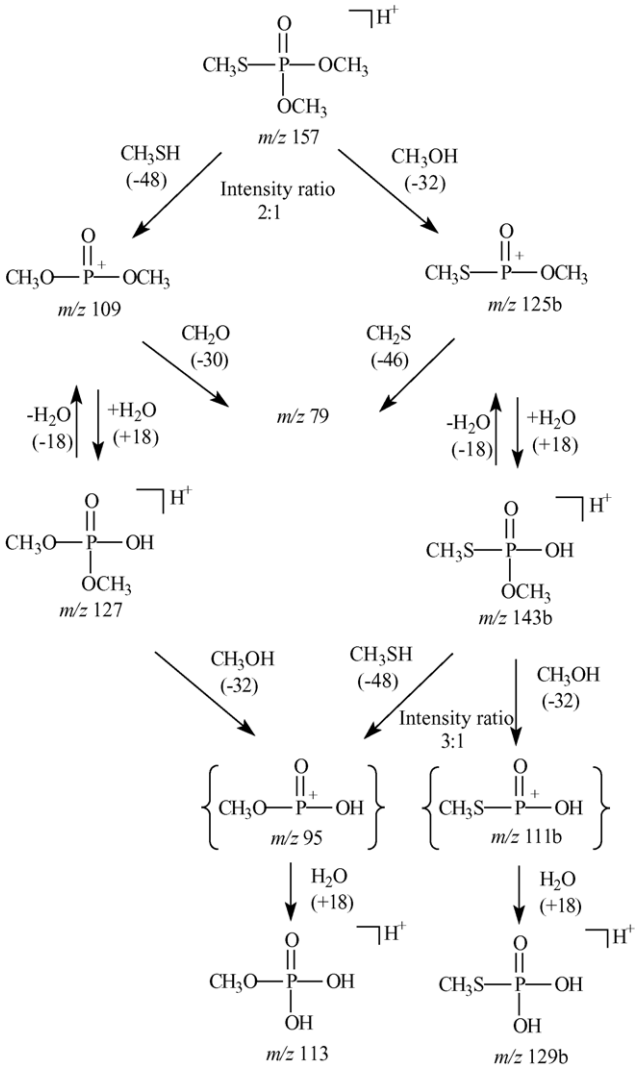

Fig. 10. Fragmentation pathways for protonated **IX**.

relative to A1. A1 is now excited to an internal energy of 200 kJ mol^{-1}. What happens? Isomerisation will occur but what about fragmentation. At first sight, since the TS to fragmentation is 300 kJ mol^{-1} relative to A1, fragmentation will not occur. But this is to ignore what happens on excitation in an ion trap. On excitation, *all* ions with a particular *m/z* will increase their internal energy relative to their unexcited or ground states by the same amount. Thus, in the case under consideration both A1 and A2, being isomers, will have their internal energies increased by 200 kJ mol^{-1} relative to their ground state, and fragmentation of A2 will occur (even though its TS to fragmentation is 300 kJ mol^{-1} relative to the starting ion, A1). In summary, the availability of TSs for all ions with *m/z* equal to that of the ions initially isolated and excited must be referenced relative to the particular isomer under consideration. This aspect was not considered in an earlier paper (reference [3]) but in retrospect does not markedly affect the arguments presented therein, although it gives an alternative or additional explanation for one particular dissociation step, **X** → **XII** + CH_2O, using the nomenclature of that paper.

4.1. Phosphonates

Fragmentation of the protonated parent phosphonates is of little interest except that of the mixed ester **III**. No transition state for the fragmentation of **III**H$^+$ has been found; bond breaking leads to two "non-interacting" molecules. Following the reaction coordinate of bond breaking via a relaxed scan (i.e., a scan in which all variables are optimised except the distance between the atoms in the bond that it is proposed to break), the total energy does not show a maximum but increases to an asymptotic value. Initially, the proton will be on the P=O (**III**H1$^+$) as the PAs for the basic sites in the thiolate **III** are 895, 828 and 788 kJ mol^{-1} for the phosphoryl oxygen, the thiol sulphur and the methoxy oxygen, respectively. For fragmentation to occur the proton needs to move to either the O (giving **III**H2$^+$) for methanol elimination or the S (giving **III**H3$^+$) for thiol elimination. In this case we see predominantly thiol elimination with only a trace of methanol being formed. As there are no TSs for the elimination of thiol or methanol, the branching ratio, i.e., their relative amounts will be determined by a combination of the endothermicity of the fragmentation and the population of the particular protomer to that fragmentation. The endothermicity should be calculated from the energy of the particular precursor protomer and not from the **III**H1$^+$ as discussed earlier. This gives endothermicities of 110 kJ mol^{-1} for methanol elimination and 171 kJ mol^{-1} for thiol elimination. If endothermicity was the main criterion for determining the branching ratio then methanol elimination should be dominant and it is not. Thus, the relative populations of the precursor protomers are important. Two things affect this—the PAs of the protomers and TS energies to access them. The TS energy to access the protomer for thiol elimination (i.e., **III**H1$^+$ → **III**H3$^+$) is 145 kJ mol^{-1} and that to access the protomer for methanol elimination (i.e., **III**H1$^+$ → **III**H2$^+$) is 171 kJ mol^{-1}. These processes are summarised in Fig. 11.

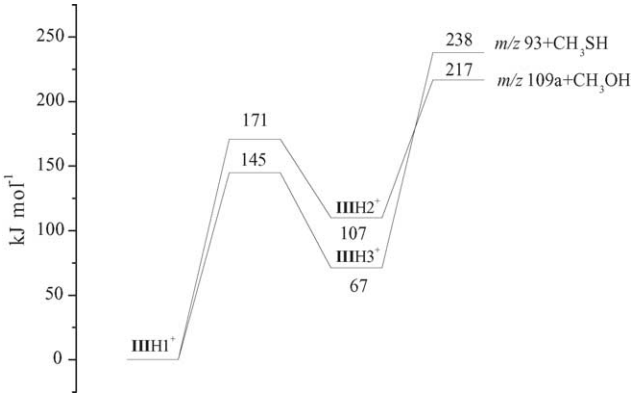

Fig. 11. Energetics in kJ mol^{-1} for the fragmentation of **III**H$^+$.

Table 1
Neutral fragmentation products of the isomeric ions with *m*/*z* 109 and 112

	Formaldehyde	Methanol	Thioformaldehyde	Thiomethanol	Other
109a $CH_3P^+(O)SCH_3$	CH_2O	CH_3OH	CH_2S	None	
112a $CD_3P^+(O)SCH_3$	CH_2O	CH_3OD	CH_2S	None	
109b $CH_3P^+(S)OCH_3$	CH_2O	CH_3OH	CH_2S	CH_3SH Trace	
112b $CH_3P^+(S)OCD_3$	CD_2O	CD_3OH	CH_2S CD_2S	CH_3SD	Trace H_2S

In the case of the ions with *m*/*z* 112, a product aligned right indicates no migration of the methyl group attached to phosphorus, whilst those aligned left migration of the methyl group from phosphorus.

The TS energy for **III**H1$^+$ → **III**H2$^+$ is comparable to the endothermicity of the fragmentation to MeSH so both processes are finely balanced, suggesting that the dominant factor in determining the branching ratio are the relative TS energies for proton migration.

The most interesting and complex fragmentations are those of the isomeric ions with *m*/*z* 109 and their isotopomers with *m*/*z* 112, the fragmentation products of which are summarised in Table 1.

Before attempting to rationalise these fragmentations, it is useful to consider the various isomers of these ions, their potential fragmentation products, and their relative energies as obtained from the electronic structure calculations. In the following discussion the superscripts 1 and 2 serve to distinguish the methyl groups (or their carbon containing moieties) and **a**–**d,** the isomeric structures (for the immediate purpose, masses of the ions, i.e., 109 or 112 have been omitted).

$^1CH_3OPS^2CH_3^+$ (**d**) $^1CH_3P(O)S^2CH_3^+$ (**a**) $^1CH_3P(S)O^2CH_3^+$ (**b**) $^1CH_3SPO^2CH_3^+$ (**c**)

When unlabelled, ions **a** and **b** give identical products (apart from a minor additional product from **b**) in similar amounts indicating that they interconvert. Electronic structure calculations show that the ions **a** and **b** are, surprisingly, close energetically. The energy of the transition state for isomerisation is 184 kJ mol^{-1} which is less than the activation energies for all but one of the possible fragmentation pathways. When unlabelled, the ions **c** and **d** (produced by 1,2Me shift from P to O or S, respectively) are the same and are 15 kJ mol^{-1} higher in energy than the ions **a** and **b**. The energy of the transition state for **b** → **c** is 218 kJ mol^{-1} above **b** and that for **a** → **d** is 241 kJ mol^{-1} above **a**. These interconversions are summarised in Fig. 12.

Based upon the H migrations and associated mechanisms found in reference [3], the likely fragmentations and associated energetics from the DFT calculations performed in this work are as follows:

		TS energies (kJ mol^{-1})	Products (kJ mol^{-1})	
$^1CH_3P(O)S^2CH_3^+$				
a	1,3H shift to P → $^1CH_3PO(H)^+ + {}^2CH_2S$	194	260	(1)
	1,4H shift to O → $^1CH_3POH^+ + {}^2CH_2S$	223	190	(2)
	1,3H shift to S → $^1CH_2PO^+ + {}^2CH_3SH$	275	426	(3)
$^1CH_3P(S)O^2CH_3^+$				
b	1,3H shift to P → $^1CH_3PS(H)^+ + {}^2CH_2O$	225	182	(4)
	1,4H shift to S → $^1CH_3PSH^+ + {}^2CH_2O$	267	159	(5)
	1,3H shift to O → $^1CH_2PS^+ + {}^2CH_3OH$	290	354	(6)
$^1CH_3SPO^2CH_3^+$				
c	1,3H shift to P → $^1CH_3SPH^+ + {}^2CH_2O$	203	204	(7)
	1,3H shift to P → $^2CH_3OPH^+ + {}^1CH_2S$	170	295	(8)
	1,4H shift to O → $^1CH_2SP^+ + {}^2CH_3OH$	261	210	(9)
	1,4H shift to S → $^2CH_2OP^+ + {}^1CH_3SH$	265	307	(10)
$^1CH_3OPS^2CH_3^+$				
d	1,3H shift to P → $^2CH_3SPH^+ + {}^1CH_2O$	203	204	(11)
	1,3H shift to P → $^1CH_3OPH^+ + {}^2CH_2S$	170	295	(12)
	1,4H shift to O → $^2CH_2SP^+ + {}^1CH_3OH$	261	210	(13)
	1,4H shift to S → $^1CH_2OP^+ + {}^2CH_3SH$	265	307	(14)

As was found earlier[3], all pathways (reactions (1)–(14)) proceed through the formation of a complex between the phosphorus containing ion and the neutral which then dissociates. It should be noted that the energies of the TSs for reactions (7)–(14) are relative to the energies of the ions **c** and **d**, although the energies of the products are referenced to the initial starting ions **a** or **b**. The ions CH_2SP^+ and CH_2OP^+ resulting from the 1,4H shifts in reactions (9), (10), (13) and

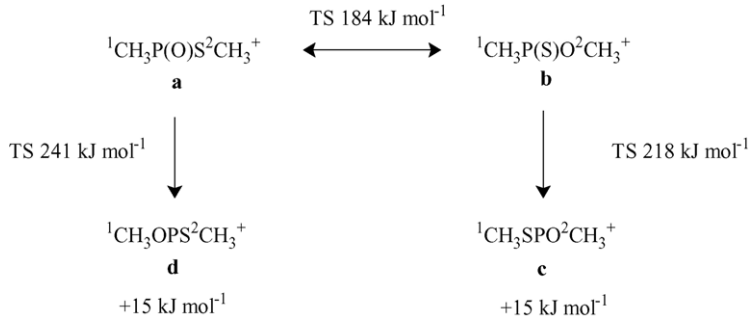

Fig. 12. Interconversions of the isomeric ions, **a**–**d**; all energies are referenced to the ions **a** and **b**.

(14) can exist in various forms, linear singlet, angular triplet and cyclic singlet. For both ions the cyclic form is the most stable.

When the ^{1}methyl and ^{2}methyl groups are both unlabelled, fragmentation of **a** gives CH_2S, CH_2O, and CH_3OH as the neutrals with intensity (branching) ratios of 5:1:4. No CH_3SH is observed. When the ^{1}methyl and ^{2}methyl are both unlabelled, fragmentation of **b** gives CH_2S, CH_2O and CH_3OH as the neutrals with intensity (branching) ratios of 4:1:4 with a trace of CH_3SH being observed. This difference, whilst small, is of considerable significance when the fragmentations of the deuterated isotopomers are considered (as will be seen later). Analysis of the derived thermodynamic values suggests that CH_2S can be formed by both reactions (1) and (8) with reaction (2) possibly making a contribution. Although reaction (12) has the same TS energy as reaction (8) it can only be accessed by the high energy TS of **a** → **d**. Similarly, both reactions (4) and (7) are likely to be pathways for CH_2O production.

Why is a trace of CH_3SH observed from **b** but not from **a**? There are two routes to CH_3SH, reactions (3) and (10) (any routes from **d** being ignored because of its relative inaccessibility). Reaction (3) has too high a TS energy (and is too endothermic) and moreover cannot be operating as, if it were, CH_3SH would be produced from **a**. The CH_3SH must therefore arise from reaction (10) and is only observed when **b** is the starting ion as **b** can isomerise directly to **c** via a relatively low energy TS. Thus that a trace of CH_3SH is observed from **b** but not from **a** is explicable in terms of kinetics. What of the formation of CH_3OH? Again there are two possible pathways, reactions (6) and (9). Reaction (6) has too high a TS energy (and is too endothermic) to be accessible. If reaction (9) was the sole pathway, the amount of CH_3OH would be expected to depend upon whether **a** or **b** was the starting ion, as is the case with CH_3SH but it does not and as the TS energies for reactions (9) and (10) are virtually identical, similar amounts of CH_3OH and CH_3SH would be expected. Since formation of CH_3OH is a major pathway with a similar branching ratio to CH_2S, it follows that the TS energy for the major pathway of its formation should be similar to that for CH_2S although a small amount is expected to be formed by reaction (9). Before alternative reaction surfaces for MeOH are explored, it is useful to consider the results obtained from the deuterated isotopomers. The arguments are not straightforward as when the ^{1}methyl is labelled with deuterium, the starting ion is **a** whereas, when the ^{2}methyl is deuterated the starting ion is **b**.

Consider first the isotopomer with ^{1}methyl deuterated. The formation of $^2CH_3OD$ supports the conclusion that CH_3OH is not formed from **d**, and must be formed either from **b** or **c**. The formation of only undeuterated $^2CH_2O$ is consistent with the suggestion that it can arise from reactions (4) and (7) and that **d** is not accessible. That only undeuterated $^2CH_2S$ is observed indicates that it is only formed by reaction (1) from **a** and not via reaction (8). That there is no observable kinetic isotope effect as reflected in the product ratios when starting with either unlabelled **a** or **a** with the ^{1}methyl deuterated, may be a reflection of the complex kinetics rather than being of profound mechanistic significance.

Consider now the isotopomer with the ^{2}methyl deuterated. Only $^2CD_2O$ is observed consistent with reactions (4) and (7) being the routes of formation for formaldehyde with **d** not being accessed. The observation of only $^2CD_3OH$ being formed again confirms the inaccessibility of **d**. Both $^2CD_2S$ and $^1CH_2S$ are produced together with a large amount (ca. 12% of the ion count) of $^1CH_3SD$. The production of $^1CH_2S$, which must arise via reaction (8) is not surprising given that much of the fragmentation must go via **c** as shown by the production of $^1CH_3SD$. The non-observation of $^1CD_2S$ from deuterated **a** is explicable in terms of kinetics as **c**, its precursor ion, can only be accessed by two consecutive isomerisations, viz **a** → **b** → **c**. That much of the reaction goes via **c** is a reflection of how close are the energies of the transitions states. An increase in the TS energy for reactions (1) and (4) due to the breaking of a C–D bond as opposed to the breaking of a C–H bond leads automatically to an increase in the amount of fragmentation going via the **c** isomer.

A good agreement between energetic considerations and the fragmentations of the isotopomers has thus been reached with the major exception of methanol production. It has been concluded either **b** or **c**, but not **d**, must be the precursor to methanol production.

The reaction pathways for methanol production investigated so far (reactions (6) and (9)) have involved a hydrogen transfer directly from the ^{1}methyl to the oxygen connected to the ^{2}methyl to produce a complex of $^2CH_3OH$ and the phosphorus containing ion which then dissociates into products.

The cyclic ion CH_2SP^+ is 124 kJ mol^{-1} lower in energy than the ion CH_2PS^+ produced in reaction (6). This cannot be produced directly starting from **b** but an alternative mechanism is to transfer a hydrogen atom from the ^{1}methyl in **b** to the phosphorus atom (a 1,2H shift C to P) followed by a further 1,2H shift from P to O which then forms the usual ion–molecule complex before dissociating into products. This gave an energetically accessible TS as shown in Fig. 13

It should be remembered that the energy of the second TS at 303 kJ mol^{-1} is referenced to the energy of **b** whereas, in reality it is reduced to 217 kJ mol^{-1} due to the increase in energy of the isomer at 86 kJ mol^{-1} resulting from the 1,2H shift from C to P. But does this alternative mechanism have its counterpart in the production of $^2CH_3SH$ from **a** or CH_3OH from $CH_3P(O)OCH_3^+$? Calculations show that the energies of the corresponding TS states for the 1,2H shift are 300 and 303 kJ mol^{-1}, respectively which corresponds with the non-observation of CH_3OH formation from $CH_3P(O)OCH_3^+$ and the formation of $^1CH_3SH$ from **c**, a more energetically accessible route for CH_3SH formation. It should be noted that the corresponding H shift from C to P for **c** leads to either $^2CH_2O$ or $^1CH_2S$ and not CH_3OH or CH_3SH.

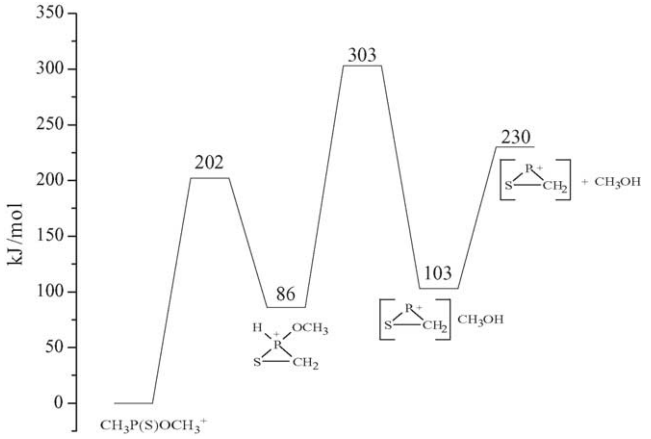

Fig. 13. Energetics in kJ mol^{-1} for the formation of $^{2}CH_3OH$ from **b,** $^{1}CH_3P(S)O^{2}CH_3^+$.

4.2. Phosphates

As for the phosphonates, of the parent compounds, only the fragmentation of the protonated mixed ester **IX** is of interest. Again, no transition state for the fragmentation of the protonated ester has been found. The energetics of the proton migrations and fragmentations are summarised in Fig. 14.

The TS energies for the proton migrations and endothermicites of the two pathways are somewhat closer together than those in the phosphonate case and so it is to be expected that a more balanced branching ratio is observed, 2:1 MeSH:MeOH. It should be noted that in estimating branching ratios from spectra such as that shown in Fig. 6, due cognizance has to be taken of the propensities of the ions with *m/z* 109 and 125b to add water, i.e., the branching ratios are determined by summing the intensities of *m/z* 109 and 125 and of *m/z* 125 and 143, respectively.

Very similar patterns of fragmentations to those observed in the phosphonate series were found. In particular the isomeric ions *m/z* 125a and b fragment to give the same product (*m/z* 79) but do not yield the same half-ester (i.e., the ions *m/z* 143a and b) on reaction with water. As for the phosphonates the two isomers have almost identical energies (*m/z* 125b being 1.8 kJ mol^{-1} below *m/z* 125a) with a TS energy of 184 kJ mol^{-1} above *m/z* 125a. This TS energy for methyl migration is the same as for the corresponding process in the phosphonates. However, unlike the phosphonate ions they only eliminate CH_2S with no CH_2O, CH_3SH or CH_3OH being produced. The energetics for the possible fragmentations and associated energetics from the DFT calculations performed in this work are as follows:

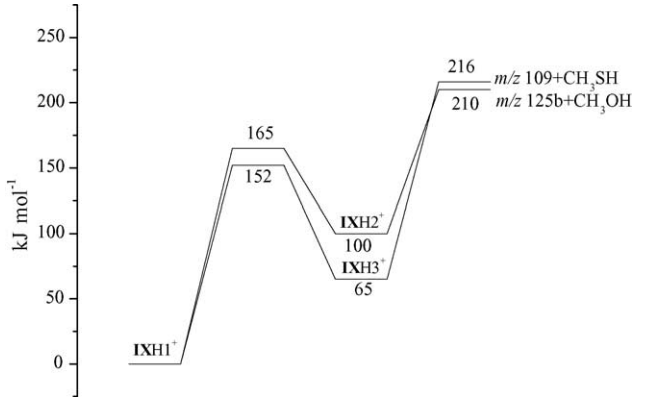

Fig. 14. Energetics in kJ mol^{-1} for the fragmentation of **IX**H$^+$.

		TS energies (kJ mol^{-1})	Products (kJ mol^{-1})	
$CH_3OP(S)OCH_3^+$				
m/z 125a	1,3H shift to P → $CH_3OP(S)H^+ + CH_2O$	251	157	(15)
	1,4H shift to S → $CH_3OPSH^+ + CH_2O$	277	108	(16)
	1,4H shift to O → $CH_2OPS^+ + CH_3OH$	358	173	(17)
$CH_3SP(O)OCH_3^+$				
m/z 125b	1,3H shift to P → $CH_3OP(O)H^+ + CH_2S$	257	235	(18)
	1,4H shift to =O → $CH_3OPOH^+ + CH_2S$	229	116	(19)
	1,4H shift to S → $CH_2OPO^+ + CH_3SH$	316	169	(20)
	1,3H shift to P → $CH_3SP(O)H^+ + CH_2O$	229	184	(21)
	1,4H shift to =O → $CH_3SPOH^+ + CH_2O$	310	89	(22)
	1,4H shift to O → $CH_2SPO^+ + CH_3OH$	333	198	(23)
$CH_3OP(O)OCH_3^+$				
	1,3H shift to P → $CH_3OP(O)H^+ + CH_2O$	219	175	(24)
	1,4H shift to =O → $CH_3OPOH^+ + CH_2O$	330	56	(25)
	1,4H shift to O → $CH_2OPO^+ + CH_3OH$	355	174	(26)

The lack of fragmentation to CH_3OH and CH_3SH is in accord with the high TS energies of the possible reactions. As was found for the phosphonates, all pathways (reactions (15)–(26)) proceed via an intermediate complex of the ionic and neutral products. The most favourable route for CH_2S production is reaction (19). This has a TS energy higher than the TS energy for interconversion of *m/z*125a and b as is expected, given that the identical fragmentation of both isomers. The major problem is the lack of production of CH_2O by reaction (21), which has the same TS energy as reaction (19). The transition states for the reactions (19) and (21) were investigated further using QST2 and QST3 methods and as well as by direct optimisation of the transition state. The same results were obtained in all cases, with an imaginary frequency corresponding to the right motion of the hydrogen atom. Alternative, lower energy, transition states for reaction (19) were sought by starting with different TS geometries but all lead to the same transition state as before. We have, at present, no explanation for this lack of correlation between the electronic structure calculations and the experimental results particularly as the agreement in all other cases is excellent.

In Fig. 10 it is seen that both *m/z* 109 and 125b give an ion with *m/z* 79. The results of the DFT calculations given above shows that the *m/z* 79 formed from *m/z* 109 results from a 1,3H shift to P whereas that formed from *m/z* 125b results from a 1,4H shift to the phosphoryl oxygen (=O).

5. Conclusions

The present studies on electrospray ionisation ion trap mass spectrometry of organophosphates of a series of dimethyl methylphosphono and trimethyl phosphoro thionates and thiolates have demonstrated that although use of deuterated isotopomers can be particularly informative a detailed understanding of the reaction pathways is only possible when the experimental approach is supported by electronic structure calculations (in the present instance at the DFT-B3LYP level). It is, however, important to point out that there is one exception in the present work, the failure to explain the fragmentation of the ion $CH_3OP(O)SCH_3^+$ which produced CH_2S but not CH_2O. Of particular interest is the comparison of the collision-induced fragmentation of ions from these compounds with those of the non-sulphur containing analogues reported previously.

Whilst ESI/ITMS is undoubtedly a powerful tool in the identification and analysis of organophosphates, the results presented here have demonstrated the complexity of the fragmentation patterns and have confirmed earlier conclusions [4] that considerable care has to be exercised in interpreting them until considerably more compounds have been examined and mechanistic rules formulated. Such studies need to be undertaken at a fundamental level as few systematic studies of the gas-phase chemistry of even electron ions from complex molecules (not just organophosphates) have been undertaken, due at least in part to the absence of suitable instrumentation before the advent of ESI/ITMS. The detailed mechanisms of some of the fragmentations only became clear from a combination of isotopic labelling and electronic structure calculations.

Of particular importance in the analytical context, is the suggestion that traces of impurities/isomers/analogues of higher proton affinity than the prime compound under investigation can dominate the ESI/ITMS spectrum. If this is confirmed it raises doubts as to the general utility of this approach for the analysis of complex mixtures such as environmental samples unless the target materials have high proton affinity. Further work in this area is therefore required.

Acknowledgements

Support from the EC “Reactive Intermediates” Research Training Network and the Leverhulme Trust is gratefully acknowledged. F.F. and G.L.M. thank the Computing Centre of the University of Palermo for providing the cluster of processors used for the quantum-chemical calculations.

References

[1] A.J. Bell, D. Despeyroux, J. Murrell, P. Watts, Int. J. Mass Spectrom. Ion Processes 165–166 (1997) 533.
[2] J.D. Barr, A.J. Bell, D.O. Konn, J. Murrell, C.M. Timperley, M.J. Waters, P. Watts, Phys. Chem. Chem. Phys. 4 (2002) 2200.
[3] A.J. Bell, A. Citra, J.M. Dyke, F. Ferrante, L. Gagliardi, P. Watts, Phys. Chem. Chem. Phys. 6 (2004) 1213.
[4] A.J. Bell, J. Murrell, C.M. Timperley, P. Watts, J. Am. Soc. Mass Spectrom. 12 (2001) 902.
[5] J.D. Barr, A.J. Bell, M. Bird, F. Ferrante, J.L. Mundy, J. Murrell, C.M. Timperley, P. Watts, J. Am. Soc. Mass Spectrom. 16 (2005) 515.
[6] M.I. Kabachnik, T.A. Mastryukova, Zh. Obshch. Khim. 25 (1955) 1867 (English translation).
[7] R.G. Pearson, J. Am. Chem. Soc. 85 (1963) 3533.
[8] A.J. Burn, J.I.G. Cadugan, J. Chem. Soc. (1961) 5532.
[9] A.J. Burn, J.I.G. Cadugan, H.N. Moulden, J. Chem. Soc. (1961) 5542.
[10] W.J. Stec, B. Uznanski, K. Bruzik, J. Michalski, J. Org. Chem. 41 (1976) 1291.
[11] M.F. Gazzard, G.L. Sainsbury, D. Sellers, D.W. Swanston, P. Watts, Biochem. Pharm. 23 (1974) 751.
[12] A. Calderbank, R. Ghosh, J. Chem. Soc. (1960) 637.
[13] T.R. Fukuto, R.L. Metcalf, J. Am. Chem. Soc. 76 (1976) 5103;
T.R. Fukuto, E.M. Stafford, J. Am. Chem. Soc. 79 (1957) 6083;
D.F. Heath, J. Chem. Soc. (1958) 1643;
F.W. Hoffmann, T.R. Moore, J. Am. Chem. Soc. 80 (1958) 1150;
A.H. Ford-Moore, G.W. Wood, Br. Patent 851 (1960) 590.
[14] W.G. Emmett, H.O. Jones, J. Chem. Soc. 99 (1911) 713.
[15] J.L. Mundy, C.M. Timperley, in preparation.
[16] R.G. Cooks, A.F. Gerrard, J. Chem. Soc. (B) (1968) 1327.
[17] E. Santoro, Org. Mass Spectrom. 7 (1973) 589.
[18] T. Kuivalainen, R. Kostiainen, H. Björk, R. Uggla, M. Sundberg, J. Am. Soc. Mass Spectrom. 6 (1995) 488.
[19] J.L. Mundy, C.M. Timperley, M.J. Waters, P. Watts, in press.
[20] M.J. Frisch, G.W. Trucks, H.B. Schlegel, G.E. Scuseria, M.A. Robb, J.R. Cheeseman, V.G. Zakrzewski, J.A. Montgomery, R.E. Stratmann, J.C. Burant, S. Dapprich, J.M. Millam, A.D. Daniels, K.N. Kudin, M.C. Strain, O. Farkas, J. Tomasi, V. Barone, M. Cossi, R. Cammi, B. Mennucci, C. Pomelli, C. Adamo, S. Cliffoird, J. Ochterski, G.A. Petersson, P.Y. Ayala, Q. Cui, K. Morokuma, D.K. Malick, A.D. Rabuck, K. Raghavachari, J.B. Foresman, J. Cioslowsli, J.V. Ortiz, B.B. Stefanov, G. Liu, A. Liashenko, P. Piskorz, L. Komaromi, R. Gomperts, R.L. Martin, D.J. Fox, T. Keith, M.A. Al-Laham, C.Y. Peng, A. Nanayakkara, C. Gonzalez, M. Challacombem, P.M. Gill, B.G. Johnson, W. Chen, M.W. Wong, J.L. Andres, M. Head-Gordon, E.S. Replogle, J.A. Pople, Gaussian 98, Gaussian Inc., Pittsburgh, PA, 1988.
[21] JANAF, http://webbook.nist.gov/.
[22] R.V. Hodges, T.J. McDonnel, J.L. Beauchamp, J. Am. Chem. Soc. 102 (1980) 1327.
[23] e.g. R.E. March, J. Mass Spectrom. 32 (1997) 35.